

Effect of Fiber Surface Treatment of Poultry Feather Fibers on the Properties of Their Polymer Matrix Composites

M. S. Huda,¹ W. F. Schmidt,² M. Misra,³ L. T. Drzal⁴

¹Product Development Department, Horticultural Research Institute, Washington, District of Columbia 20005

²USDA/ARS/ANRI/EMFSL, Beltsville, Maryland 20705

³School of Engineering, University of Guelph, Guelph, Ontario, Canada N1G 2W1

⁴Chemical Engineering & Materials Science Department, Michigan State University, East Lansing, Michigan 48824

Correspondence to: M. S. Huda (E-mail: Masud.huda@ars.usda.gov)

ABSTRACT: This study develops the enabling technology needed to transform the fibers of poultry feather (FPF), a waste product left over after processing poultry in the food processing industry, as reinforcement filler material for manufacturing composite materials. We successfully fabricated composite materials from biopolymers (polylactide, PLA) and FPF that were produced by the extruder system. FPF-reinforced polypropylene (PP) composites were also compounded and molded and compared to PLA/FPF composite. The composites were evaluated via thermal and mechanical analysis. To enhance the adhesion between the polymer matrix and the FPF, the FPF have been treated with sodium hydroxide, 10% maleinized polybutadiene rubber, and a silane-coupling agent. X-ray photoelectron spectroscopy was used to analyze the influence of modifications on the properties of fibers and found that the coupling agent was localized at the surface of the fibers. Thermal behavior of pretreated fibers was also studied by thermogravimetric analysis. All treatments clearly enhanced thermal performance of fibers. This enhancement of fiber properties, along with an improvement in fiber/matrix adhesion, led to improvement in the mechanical properties of the composite materials. It was found that the surface-treated fiber-reinforced materials offered superior mechanical properties compared to untreated fiber-reinforced composite materials. Moreover, morphological studies by the scanning electron microscopy demonstrated that better adhesion between the fiber and the matrix was achieved especially for the surface-treated fiber-reinforced composite materials. © 2012 Wiley Periodicals, Inc. *J. Appl. Polym. Sci.* 000: 000–000, 2012

KEYWORDS: biofibers; biomaterials; biopolymers and renewable polymers; composites; processing

Received 17 March 2011; accepted 1 July 2012; published online

DOI: 10.1002/app.38306

INTRODUCTION

Recently, the use of bio/natural fibers has become the subject of extensive research for the manufacture of the structural as well as semistructural fiber-reinforced thermoplastics.^{1–4} Furthermore, the fiber-reinforced polymer composites have high performance in terms of mechanical properties, significant processing advantages, low density, and low cost.^{1,2} Research is being generated mainly on the potential use of natural fibers as reinforcements for polymers, because natural fibers offer many advantages,^{1,2} such as biodegradability, abundant renewable source, flexibility during processing, low cost, desirable fiber aspect ratio, low density, and reduced wear of the processing machinery. However, materials scientists nowadays look for new fiber sources, not only for environmental reasons, but for the interesting properties that some natural products present. One very interesting possibility is keratin fiber, an animal-based nat-

ural fiber, which is obtained from poultry feathers. Its intrinsic properties have made it worthy topic to study.^{5–7} The main purpose of this study is to develop the enabling technology that is needed to transform fibers of poultry feather (FPF) into value-added products for biocomposite manufacturing.

In spite of FPF have several distinctive features that include surface toughness, flexibility, a highly organized morphology characterized by its complex hierarchical structure, high length to diameter ratio, and hydrophobicity, billions of pounds of waste feathers are generated each year by poultry processing plants creating a serious waste problem.^{5–9} Materials derived from FPF could be used advantageously in biodegradable material applications, due to the mixed hydrophobic/hydrophilic surface chemistry makes poultry fibers at least partially compatible with all polymers that are usually predominantly hydrophilic or hydrophobic,^{5,7} and keratin fibers are not only a renewable and

self-sustainable material but also ecologic, that is, biodegradable, due to their natural biopolymer origin.^{7,8} Such applications could potentially consume the 5 billion pounds of feathers produced annually as a by-product of the U.S. poultry industry.

Biopolymers such as polylactide (PLA) can be obtained from renewable resources by microbial fermentation.² Although PLA has mechanical properties suited for industrial plastic applications, it is considered too brittle for many commercial applications.^{2,3} This could be overcome by combining it with other filler materials. The properties of the interface between the fiber/filler and matrix are critical to many properties of the composite material. Much attention has been given in the past to the modification of the fibers by physical and chemical methods.^{1–3} The mixed hydrophobic/hydrophilic surface chemistry might make FPF as attractive and suitable reinforcement filler material for manufacturing PLA-based composite materials, where an additional benefit of FPF as the filler is the reduction in the overall cost of biocomposite.

In the present study, the FPF-reinforced composites were processed by the twin-screw extruder with a FPF content of 30 wt %. Usually, matrix-fiber interaction can be improved by surface or structural modification of the fibers by using the coupling agent, and the coupling agent improves the degree of cross-linking in the interface region and offers a suitable bonding result, as well as the creation of high fiber surface area, which is required for the optimization of fiber-resin reinforcement.³ In this study, FPF had been treated with sodium hydroxide and 3-aminopropyltriethoxysilane (APS)-coupling agent.¹⁰ As part of our continuing interest in preparing PLA-based composite materials showing high performance, the present work also indicates the use of maleinized polybutadiene rubber as a coupling agent in FPF-reinforced composites. In the recent years, graft copolymers of maleic anhydride (MA) with synthetic and natural polymers have been studied, and the graft copolymerization of maleic hydride onto the natural rubber molecules was carried out in molten¹¹ or solution states.¹² Hristov et al.¹³ investigated the effects of poly(butadiene styrene) rubber and maleated polypropylene used as impact modifier and compatibilizer, respectively, in the case of polypropylene (PP)/wood fiber composites. Carlson et al.¹⁴ investigated the production of maleated PLA by reactive extrusion. These authors demonstrated that improved interfacial adhesion could be obtained in PLA/starch blends through modification of PLA with low levels of MA. In this study, it was possible to prepare FPF-reinforced PLA composites by extrusion in nearly the same way as PP. The FPF-reinforced PP composite was also compounded and molded with a fiber content of 30 wt % and compared to PLA/FPF composite. Because the aim of this research was to improve the interfacial properties between the PLA matrix and the reinforcing fibers, three surface treatment methods had been tested: (i) FPF treated with an aqueous alkaline solution (FPFNA), (ii) FPF treated with a silane-coupling agent (FPFSIL), and (iii) FPF treated with maleinized polybutadiene rubber (FPFR). After analyzing the influence of these modifications on the chemical, physical, and thermal properties of FPF, the mechanical and thermal properties of their biocomposite materials were studied. This study could be an interesting step toward the development

of the biodegradable composite, which is acceptable for applications that do not require high-load-bearing capability.

EXPERIMENTAL

Materials

PLA, a corn-based polymer (product name PLA 3001D), was purchased from NatureWorks LLC, Blair, NE. The density of the PLA resin was 1.25 g/cm³. The weight-average molecular weight was about 160,000–220,000 Da. It was dried at 65°C for a minimum of 8 h before use in a desiccating dryer. PP (ProFax 6523) was obtained from Basell Polyolefins, Elkton, MD.

FPF were purchased by Featherfiber Corporation, Nixa, MO. Scanning electron microscopy (SEM) of feather material was showing the fibrous structure: length: ~3 – ~9 mm and diameter: 6–14 μm. The density of the FPF was measured to be 0.87 g/cm³. 3-APS was purchased from Gelest, Morrisville, PA. Polybutadiene functionalized with MA (Ricon 130MA13) was purchased from Sartomer USA, LLC., Exton, PA.

Fiber Surface Modification

Processing of Alkali-Treated FPF. FPF were immersed in sodium hydroxide solution (5% w/v) for 2 h at room temperature. The fibers were then washed with distilled water containing a few drops of acetic acid followed by distilled water until the NaOH was removed, that is until the rinse water no longer indicated any alkalinity.^{15,16} After washing, the fiber was air dried for 2 days. Next, the fiber was kept in an oven at 80°C for 6 h.

Processing of Silane-Treated FPF. About 5 wt % silane (3-APS; weight percentage regarding the feather fiber) was hydrolyzed in a mixture of water and ethanol (40 : 60 w/w). During surface treatment, APS hydrolyzes and the resultant silanol groups can bond with the fiber surface.¹⁰ Amine groups from APS can form hydrogen bonds to COO sites on the hydrolyzed PLA backbone. The pH of the solution was adjusted to four with acetic acid and stirred continuously for 1 h. The fibers were soaked in this solution and left for 3 h. The fibers were then washed and air-dried for 3 days. Last, the fibers were dried in an oven at 80°C for 12 h. The silane-coupling agents have ethoxy groups that are hydrolyzed in the presence of water producing silanol groups.¹⁵ APS has three ethoxy groups that yield three hydroxyl groups after hydrolysis. The silanol can then react with the OH groups on FPF, which forms stable covalent bonds to the cell wall that are chemisorbed onto the fiber surface.^{15,16} The silanols are also capable of linking with the matrix polymer through the siloxane bonds.¹⁷ Thus, the silanes act as connector molecules between the matrix and the fiber.

Processing of 10% Maleinized Polybutadiene Rubber-Treated FPF. FPF were treated with 10% polybutadiene functionalized with MA that was used as an impact modifier.¹⁸ The maleinized polybutadiene rubber was dissolved in hexane by continuously stirring using a magnetic stir bar. The solution was sprayed to feather fibers. The treated feather fibers were dried under the hood for 8 h. The fibers were then dried in a vacuum oven at 80°C for 12 h. They were then dried in an oven for 4 h at 80°C.

Table I. Surface Characterization of FPF Using X-Ray Photon Spectroscopy

Samples	Elemental Compositions (%)						Si/O ratio	O/C ratio
	C	O	N	Ca	Si			
Untreated FPF	86.01	10.11	2.67	0.53	0.69	0.068	0.118	
FPFNA	82.48	11.95	3.52	0.78	1.27	0.106	0.139	
FPFSIL	83.07	11.87	2.31	0.76	1.99	0.167	0.142	
FPFR	86.15	9.68	2.44	-	1.74	0.179	0.112	

Fabrication of Composites by Twin-Screw Extruder. Before processing, the PLA was dried under vacuum at 80°C for 24 h. The PP matrix, however, was not dried. The required amount of the fibers and the polymer was mechanically mixed in a kitchen mixer (Hamilton Beach, Model: 56200, Type: B17). Then the samples were extruded at 100 rpm with a Micro 15 cc compounding system (DSM Research, Geleen, the Netherlands) at 177°C for 10 min. The extruder has a screw length of 150 mm, an L/D of 18, and a net capacity of 15 cm³. To obtain the desired specimen samples of the PLA-based composite for various measurements and analysis, the molten composite samples were transferred after extrusion, through a preheated cylinder to an injection molder, which was preset with the injection temperature at 177°C and the mold temperature at 40°C. The density of the composite was measured to be 1.01 g/cm³, which was less than the density of neat PLA. In the case of the PP-based composite, compounding was carried out at a screw speed of 100 rpm, and extruder temperatures were set at 173°C. Injection-molded samples were placed in sealed polyethylene bags in order to prevent moisture absorption.

Testing and Characterizations

X-Ray Photoelectron Spectroscopy. The X-ray photoelectron spectroscopy (XPS) surface chemical characterization was carried out by a Physical Electronics (PHI 5400 ESCA system) electron spectrometer using a polychromatic Mg anode. The X-ray source operates at 5 kV and 300 W. The take-off angle is held at 45°. Atomic concentrations are determined by sensitivity factors supplied by the manufacturer. The analysis of the spectra was performed using commercial curve-fitting software.

Thermogravimetric Analysis. The thermogravimetric analysis (TGA) was carried out in a TA 2950 TGA. The samples were scanned from 25 to 500°C at 20°C per min in the presence of nitrogen.

Mechanical Testing. A mechanical testing machine, United Calibration Corp SFM 20, was used to measure the flexural properties according to ASTM D 790 standard and the tensile properties according to ASTM D 638 standard. System control and data analysis were performed using Datum software. The notched Izod impact strength was measured with a Monitor/Impact machine of Testing Machines (TMI) 43-02-01 according to ASTM D 256. All results presented are the average values of five measurements.

Differential Scanning Calorimeter. The melting and crystallization behavior of the matrix polymer and the composites were

studied using a TA Instruments 2920 Modulated Differential Scanning Calorimeter (DSC) equipped with a cooling attachment under nitrogen atmosphere. The data were collected by heating the composite specimen from 25 to 200°C at a constant heating rate of 5°C/min. A sample weight of ~10 mg was used. The samples were sealed in aluminum pans, and the sealed samples were placed on a heating surface in the furnace along with an empty reference aluminum pan. The heat flow and energy changes in and out of the samples in the sealed aluminum pans were recorded with reference to an empty aluminum pan. Melting temperature was obtained from the peak in the heating curve.

Scanning Electron Microscopy. The morphology of impact fracture surfaces of the composites was observed by scanning electron microscopy (SEM) at room temperature. A JEOL (model JSM-6300F) SEM with field emission gun and accelerating voltage of 10 kV was used to collect SEM images for the composite specimen. A gold coating of a few nanometers in thickness was coated on impact fracture surfaces. The samples were viewed perpendicular to the fractured surface.

RESULTS AND DISCUSSION

Elemental Composition of FPF

XPS spectra were taken of the FPF following each treatment is given in Table I. These XPS scans revealed the presence of carbon, oxygen, nitrogen, calcium, and silicon on the untreated and treated feather fiber surface. Changes in oxygen/carbon atomic ratio as a function of each treatment are shown in Table I. After silane treatment, there is a marked increase in silicon as well as oxygen contents and a decrease in carbon and nitrogen contents. After NaOH treatment, the oxygen, nitrogen, calcium, and silicon contents increase, while carbon content decreases on the surface of feather fibers. The increased O/C atomic ratio (or decreased concentration of unoxidized carbon) reduced from the aliphatic hydrocarbon chains ($-\text{CH}_2-$)_n serve to attach the functional groups to the silicon atom. The silane-treated FPF has higher Si/O atomic ratios than the NaOH-treated FPF. In addition, the increase in oxygen to carbon atom ratio of fiber surface as shown in Table I is a relative scale for increase in hydroxyl group content, which may help to increase the interaction between FPF and polymer matrix.¹⁶ According to Ullah et al.,⁴ the FPF is semicrystalline, and the crystalline phase consists of α -helical protein braided into microfibrils where the protein matrix is fixed by intermolecular interactions, especially hydrogen bonds; and in this type of protein, hydrogen bonds are many and strong.

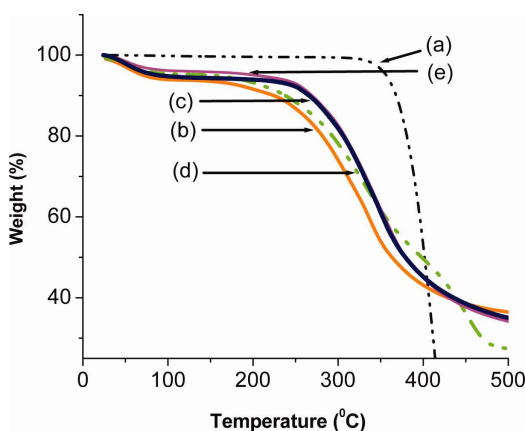


Figure 1. Thermogravimetric curves for (a) neat PLA resin, (b) untreated FPF, (c) FPF/SIL, (d) FPF/R, and (e) FPF/NA. [Color figure can be viewed in the online issue, which is available at wileyonlinelibrary.com.]

Thermogravimetric Properties

The thermal properties of the neat PLA resin and untreated- and surface treated-FPF were investigated with TGA. TGA curves as a function of temperature of neat PLA resin and untreated- and surface treated-FPF are shown in Figure 1. In Table II, the 5, 10, 25, and 50% weight-loss temperatures (T_5 , T_{10} , T_{25} , and T_{50} , respectively) are listed for all specimens shown in Figure 1. As seen in Figure 1, there are three stages to degrade the FPF: (a) the moisture absorbed during storage is released from the FPF first, (b) between 235 and 360°C, a second transition occurs, where FPF undergoes degradation, and (c) FPF starts to decompose from 360°C onward. At 200°C, 6.1, 6.9, and 4.9% weight loss were observed for FPF/SIL, FPF/R, and FPF/NA, respectively. For the untreated FPF, 8.5% weight loss was observed at 200°C. It was also observed that the weight loss of untreated FPF sample is relatively high in comparison with the surface-treated samples as seen in Table I. After the NaOH- or silane treatments, the temperature at the maximum rate of decomposition of FPF increased, indicating that this NaOH- or silane treatment leads an improvement in thermal stability.

Mechanical Properties

Flexural Properties of the Composites. Figure 2 shows the flexural strength and modulus of untreated and surface-treated FPF-reinforced composites. All surface-untreated or -treated FPF showed the tendency to significantly increase the flexural modulus of reinforced composites in comparison with the neat PLA. The chemical treatments have a lasting effect on the me-

Table II. TGA Characterization of the Neat PLA Resin and Untreated- and Surface Treated-FPF

Samples (wt %)	T_5 (°C)	T_{10} (°C)	T_{25} (°C)	T_{50} (°C)
Neat PLA resin	356	368	385	401
Untreated FPF	71	224	297	363
FPF/SIL	89	265	319	378
FPF/R	149	237	310	398
FPF/NA	203	269	321	380

chanical behavior of FPF, especially on fiber stiffness. As seen in Figure 2, the modulus of both PLA- and PP-based composites increases significantly with the addition of the surface-treated FPF. In the case of 30 wt % FPF content in PP-based composite samples, the flexural modulus is increased from 2.4 GPa for the untreated fibers to 2.9 GPa for the alkali-treated fibers, that is, a 20% increase. The composite with NaOH-treated FPF showed higher increase in modulus than that of silane-treated FPF-reinforced composite. It was also found that the flexural modulus improved significantly (improved 12%) when silane-treated feather fibers were used compared to untreated versions. Sreekala et al.¹⁷ suggested that the silane-treated cellulose fiber composite was observed to show an increase in nucleation density compared to the composite with the untreated fibers under the same conditions. The increased nucleation provided smaller crystals that result in a transcrystalline interphase region, with improved bonding between the fiber and the matrix.^{18,19} A significant increase in both flexural strength and flexural modulus of PP-based composite was observed after rubber treatment of FPF. As seen in Figure 2, the flexural modulus of every PLA/FPF composite sample in the experiments is higher than that of neat PLA sample. According to Shibata et al.²⁰ though flexural moduli increased for PLA composites, flexural strength did not increase regardless of the fiber treatment. Tests with different surface-untreated or -treated FPF-reinforced PLA composites showed that the flexural properties of these biocomposites were clearly influenced by the chemical modification of FPF that effectively resulting in improved adhesion between fiber and matrix. Lanzilotta et al.²¹ discovered that the mechanical strength of injection-molded PLA was not improved when 20–40 wt % flax was incorporated, and the authors attributed this to poor adhesion between the flax and PLA, in which PLA had been modified with MA by reactive extrusion.

Tensile Properties of the Composites. The tensile properties of the thermoplastic matrix along with PLA- and PP-based composites are shown in Figure 3. Tensile modulus increased significantly with the addition of the 30 wt % FPF, whereas tensile strength decreased slightly in the cases of the PLA-based composites. This reveals that the incorporation of the bio-/natural

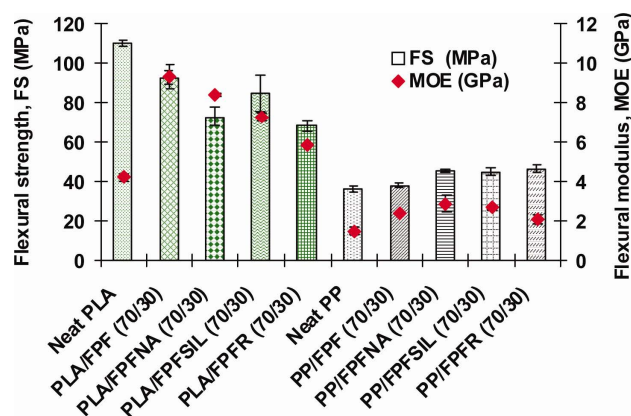


Figure 2. Flexural properties of the FPF-reinforced composites. [Color figure can be viewed in the online issue, which is available at wileyonlinelibrary.com.]

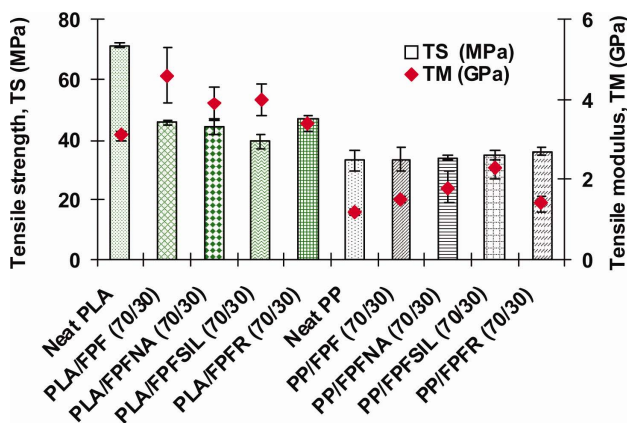


Figure 3. Tensile properties of the FPF-reinforced composites. [Color figure can be viewed in the online issue, which is available at www.interscience.wiley.com.]

fibers into the matrix provides effective reinforcement. Both tensile strength and modulus of the PP-based composites were also increased, which indicates improved adhesion between FPF and the PP matrix. In context, according to Bullions et al.,²² feather fibers were reported to improve the stiffness but reduce the breaking stress of polyethylene composites. It was reported in Bullions et al.²³ that feathers fibers provided inferior properties compared to cellulose fibers, and modulus of the composites was adversely affected by feather fibers, when feather fibers were mixed with cellulose fiber and PP matrix in a wet lay paper making process to develop composites. In the case of 30 wt % FPF content in PLA-based composite samples, the decrease in tensile strength with a high content of bio-/natural fiber is probably due to either the filler effect or insufficient hydrogen bonding between the thermoplastic matrix and the bio-/natural fibers.^{24,25} The tensile strength is more sensitive to the matrix properties, whereas the modulus is dependent on the fiber properties. Plackett²⁶ reported that the addition of PLA modified with MA (MAPLA) decreased the tensile strength of compression-molded PLA/jute composite. Plackett²⁶ suggested that PLA mechanical properties are closely correlated with molecular weight, and mechanical testing of PLA/jute composites showed a reduction in mechanical strength resulting from addition of maleated PLA to the fibers. Beckermann et al.²⁷ suggested that the incorporation of fibers into thermoplastics leads to poor dispersion of fibers due to strong interfiber hydrogen bonding, which holds the fibers together. Improper adhesion hinders the considerable increment of tensile strength. Because of the presence of hydroxyl and other polar groups in various constituents of FPF, the moisture uptake is high for dry fibers.⁸ All these lead to poor wettability with matrix and weak interfacial bonding between the FPF and hydrophobic matrix.

Figure 3 shows that the tensile modulus of every FPF-reinforced PLA composite is higher than that of neat PLA sample, and a maximum value of 4.6 GPa (increment of 48%) is reached for the FPF-reinforced PLA composite sample with FPF content of 30 wt %, although the tensile strength of the untreated- and NaOH treated- FPF-reinforced PLA composites was lower than those of the PLA matrix itself. It can be observed that the rub-

ber-treated FPF-reinforced composite shows lower modulus and higher tensile strength than other surface-treated composites. Usually, the orientation of fibers in the composites influences the tensile strength. The better fibers are aligned, the higher strength values can be obtained.¹⁵ The FPF have high aspect ratios and contribute to an increase in the moduli of the composites and can also improve the strength of the composite when suitable additives are used to improve stress transfer between the matrix and the FPF.^{4,7}

Notched Izod Impact Strength of the Composites. Figure 4 shows the impact strength of the surface-untreated or treated FPF-reinforced composites. Compared to the untreated fiber composite having 30% by weight fiber loading, the surface treatments significantly enhanced the impact strength of the composites. It is well known that the impact response of fiber composites is highly influenced by the interfacial bond strength, the matrix, and fiber properties. The impact properties of surface-treated FPF composites present an evident increase compared to untreated fiber composites. Dupraz et al.¹⁰ suggested that APS has the ability to bond to PLA. During surface treatment, APS hydrolyzes, and the resultant silanol groups can bond with the FPF surface. Amine groups from APS can form hydrogen bonds to COO-sites on the hydrolyzed PLA backbone.¹⁰ In the case of hydroxyapatite (HAP)/PLA composites, Zhang et al.²⁸ used silane derivatives as modification molecules to shield degradation of the hydroxyl groups of HAP surfaces to the polymer main chain that was carried out via direct reactions of —OR groups of the silane derivatives with —OH groups on HAP surfaces. Zhang et al.²⁸ also indicated that other functional groups (—NH₂, etc.) of the silane derivatives may further react toward the terminal groups, carboxylic groups or hydroxyl groups, of PLA at the same time. Thus, PLA can be bonded chemically to HAP surfaces by silane-coupling agents.

As seen from Figure 4, the impact strength properties of untreated- and treated FPF-reinforced PP composites were significantly higher than those of the PP matrix itself. In the presence of rubber-treated fiber-reinforced PP-based composite, the impact strength of the composite improved 77%, which may be related to the better interfacial adhesion between PP matrix polymer and rubber-treated feather fiber. For the FPFSIL-

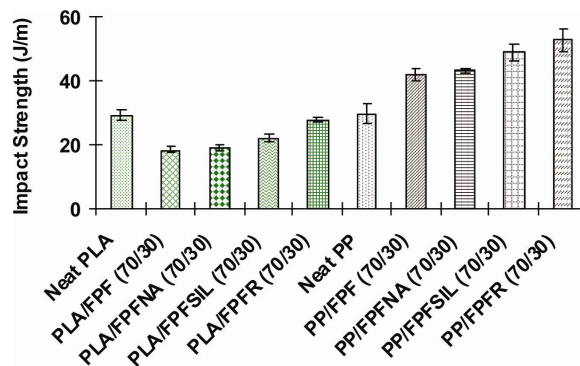


Figure 4. Notched Izod impact strength of FPF-reinforced composites. [Color figure can be viewed in the online issue, which is available at www.interscience.wiley.com.]

Table III. Thermal Properties of Neat PLA and PLA-Based Composites

Polymer/ fibers (wt %)	T_g (°C)	T_c (°C)	ΔH_c (J/g)	ΔH_m (J/g)	χ (%)	T_m (°C)
Neat PLA	57	103	30.2	41.9	44.7	172
PLA/untreated FPF (70/30)	47	81	20.0	39.4	42.0	167
PLA/FPFNA (70/30)	48	84	20.5	39.3	41.9	168
PLA/FPFSIL (70/30)	55	87	20.4	46.4	49.5	169
PLA/FPFR (70/30)	51	79	18.9	36.8	39.2	170

reinforced PP-based composite, impact strength increased significantly (64% improvement) compared to the untreated version at the same fiber content. Maleinized polybutadiene rubber noticeably improves the adhesion between the FPF and matrix forming an interfacial layer, therefore, a large increase of the impact strength in the PP-based composite. For the FPFNA-reinforced composites, slightly lower trend was observed (46% improvement). The reason is not clear, although it may be related to the better interfacial adhesion between the matrix polymer and fiber, which is more important at high fiber loading. Generally, the impact properties of composite materials are directly related to its overall toughness, where impact strength illustrates the ability of a material to resist the fracture under stress applied at high speed. The predominant mechanism of energy absorption is through crack propagation in the notched Izod test. In this study, the composite processing method played an important role on the impact properties of the FPF-reinforced composites. Although the impact strength properties of untreated- and FPFNA-reinforced PLA composites were lower than those of the PLA matrix itself, surface properties of feather fibers can be modified in terms of both silane and rubber treatments as characterized by an increased surface energy that improves wettability of the FPF when compounding with PLA.

Crystallization and Melting Behavior of the Composites

The thermal characteristics of the composites were investigated via DSC. The glass transition temperature (T_g), crystallization temperature (T_c), melting temperature (T_m), crystallization enthalpy (ΔH_c), and melting enthalpy (ΔH_m) obtained from the DSC studies are summarized in Table III. Using literature reference values for the PLA melting enthalpies, under the assumption that the polymer is purely crystalline, it was possible to obtain the degree of crystallinity (χ %) in the composite, $\chi = \Delta H_m / \Delta H_m^0 \times 100$, where ΔH_m is the experimental melting enthalpy (J/g) and ΔH_m^0 the melting enthalpy of a pure crystalline matrix, PLA (93.7 J/g).²⁹

Table III indicates that the T_g and T_m of the composites changed with the addition of FPF to the PLA matrix. Both untreated and treated-feather fiber-filled PLA composite shows an decrease in T_g compared to neat PLA. These observations indicate that the composite changed from tough to flexible properties.³⁰ The melting enthalpy, crystallization enthalpy, crystallization temperature, and degree of crystallinity of the PLA composites decreased for the presence of untreated or treated FPF in the case of PLA/FPF composites though same trend did not follow

in the case of silane-treated FPF-reinforced PLA composite. These results suggest that both treated and untreated FPF affect the crystallization properties of the PLA matrix. The crystallization temperature of the PLA/FPF composite decreased by up to 22°C when compared with neat PLA, which signifies that the treated feather fibers hinder the migration and diffusion of PLA molecular chains to the surface of the nucleus in the composites.^{16,31} Similar results were obtained in the case of PLA/FPFNA composite. According to Krassig³² and Rana et al.,³³ there are two main factors controlling the crystallization of polymeric composite systems: (i) additives having a nucleating effect that results in an increased crystallization temperature, which increases crystallinity, and (ii) additives hindering the migration and diffusion of polymer chains to the surface of the growing polymer crystal, resulting in a decrease in the crystallization temperature, lowering crystallinity. The crystallinity was found to decrease as a result of the addition of FPFR in the case of PLA/FPFR (70/30) composite. The crystallization temperature of PLA decreased by ~5°C when FPFR was added. Shih et al.³ reported that the values of the melting enthalpy were decreased with the addition of the surface chemically modified recycled disposable chopsticks fiber (MRDCF). According to Fornes and Paul,³⁴ it indicates that the MRDCF may disrupt the crystallite formation of PLA and lead to less-ordered crystals and smaller crystallinity of the composites when compared with the pristine PLA.

Morphology of FPF and FPF-Reinforced PLA Composites

The effects of the different treatments on the surface fiber and the adhesion between matrix and FPF were investigated by SEM. SEM micrographs of the fracture surface of the untreated FPF reinforced PLA composites can be seen in Figure 5(a, b). These figures show the presence of aggregation of the untreated FPF at the surface. Zooming in on the fibers reveals that there are voids in the polymer matrix around the fibers as well as voids in the polymer—matrix where fibers once resided. In Figure 5(b), the fiber pull-out in the micrographs is an indication of low-fiber/matrix adhesion.

SEM micrographs of the fracture surface of the treated FPF-reinforced PLA composites can be seen in Figure 5(c–f). SEM micrographs of the treated composites in these figures show the variability in matrix-FPF adhesion for the treated and untreated composites, and it is clearly indicated higher interfacial shear strength for treated fibers and good interfacial adhesion between the fibers and matrix. SEM images of the FPFNA-reinforced PLA composites in Figure 5(c, d) show fewer holes than observed in untreated fibers. As seen in Figure 5(d), NaOH treatment facilitates good adhesion between FPF and PLA matrix, and it may be that the fiber surface is rougher than in the untreated FPF fiber composites, which contributes to the enhancement of the bonding strength between fiber and matrix. Figure 5(e, f) of the FPFSIL-reinforced PLA composites show that FPF are well trapped by the PLA matrix. It implies that the changes of surface topography affect the interfacial adhesion. In Figure 5(f), the presence of silane produces better fiber dispersion, and this morphology is optimal for toughening to occur. From the SEM micrographs, we can say that the surface treatment of FPF has improved the adhesion between fiber and

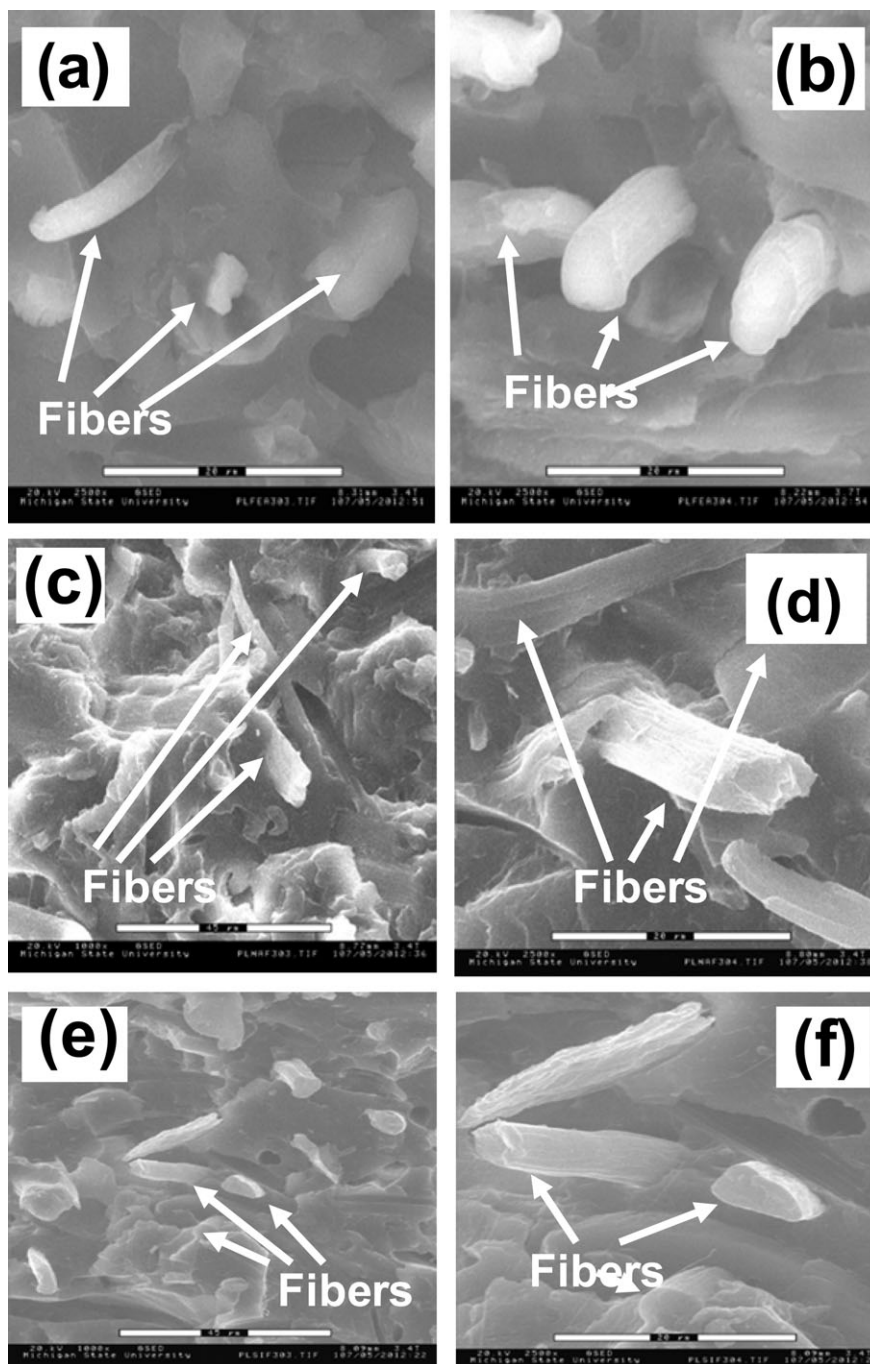


Figure 5. SEM micrographs of the impact fracture surface of (I) PLA/untreated PPF (70 wt %/30 wt %) composite: (a) 20 and (b) 20 μm ; (II) PLA/FPFNA (70 wt %/30 wt %) composite: (c) 40 and (d) 20 μm ; and (III) PLA/FPFSIL (70 wt %/30 wt %) composite: (e) 40 and (f) 20 μm .

matrix, which in turn improved the mechanical properties. The result of the treatments is that FPF increase their potential use as reinforcing agent for polymeric composite materials.

CONCLUSIONS

This study demonstrated that an environmentally friendly composite with good mechanical and thermomechanical properties could be successfully developed using FPF as a reinforcing agent

and PLA as a matrix. The main disadvantage of bio/natural fibers in thermoplastics is the poor compatibility between the fibers and matrix. Therefore, surface treatments were used to modify the properties of poultry feather fibers. It was found by XPS analysis that the coupling agent was localized at the surface of the fibers. Thermal behavior of pretreated FPF was also studied by TGA, and both treatments clearly enhanced thermal performance of fibers. This enhancement of fiber properties, along with an improvement in fiber/matrix adhesion, led to

improvement in the mechanical properties of the composites, specially in the case of PP composites. The results of the study showed that silane-coupling agent improves the compatibility between FPF and PLA resin. This is believed to be caused by improved interfacial interaction, resulting in high stiffness. The mechanical properties of the fiber-reinforced PLA composites were found to compare favorably with the corresponding properties of PP composites. Surface-treated FPF composites possessed superior mechanical properties to composites made from as-received fibers. The reinforcement of neat polymer matrix by means of treated FPF significantly improves stiffness. The SEM photographs of fracture surfaces of composites clearly indicated the extent of fiber-matrix interface adhesion. It may be concluded that surface-treated FPF and polymer matrix can be molded into a value-added composite material by using the molding method. Moreover, further research works have been carried to establish the multiple formulations for the development for biodegradable materials from FPF by using biodegradable additives that were also successfully extruded, and now these multiple formulations are presently optimizing processes and still evaluating the materials properties of the end products. Further investigations have to be carried out to determine the biodegradability of these composites.

REFERENCES

- Saheb, D. N.; Jog, J. P. *Adv. Polym. Technol.* **1999**, *18*, 351.
- Plackett, D.; Logstrup, A. T.; Batsberg, P. W.; Nielsen, L. *Compos. Sci. Technol.* **2003**, *63*, 1287.
- Shih, Y. F.; Huang, C. C.; Chen, P. W. *Mater. Sci. Eng. A* **2010**, *527*, 1516.
- Ullah, A.; Thavaratnam, V.; David, B.; Elias, A.; Wu, J. *Bio-macromolecules* **2011**, *12*, 3826.
- Verbeek, C. J. R.; Berg, L. E. V. *Macromol. Mater. Eng.* **2010**, *295*, 10.
- Reddy, N.; Yang, Y. J. *Polym. Environ.* **2007**, *15*, 81.
- Misra, M.; Kar, P.; Priyadarshan, G. MRS Symposium Proceedings, December, Boston, MA, **2001**; 702, p 35.
- Fraser, R. D. B.; MacRae, T. P.; Rogers, G. E. *Keratins: Their Composition, Structure, and Biosynthesis*; Charles C. Thomas: Springfield, **1972**; p 31.
- Bonser, R. H. C.; Purslow, P. P. *J. Exp. Biol.* **1995**, *198*, 1029.
- Dupraz, A. M. P.; de Wijn, V. D. Jr.; de Groot Meer, K. S. A. T. *J. Biomed. Mater. Res.* **1996**, *30*, 231.
- Nakason, C.; Kaesman, A.; Homsin, S.; Kiatkamjornwong, S. *J. Appl. Polym. Sci.* **2001**, *81*, 2803.
- Visconte, L. L. Y.; Andrade, C. T.; Azuma, J. *Appl. Polym. Sci.* **1997**, *69*, 907.
- Hristov, V. N.; Lach, R.; Grellmann, W. *Polym. Test.* **2004**, *23*, 581.
- Carlson, D.; Nie, L.; Narayan, R.; Dubois, P. *J. Appl. Polym. Sci.* **1999**, *72*, 477.
- Joseph, S.; Sreekala, M. S.; Thomas, S. *J. Appl. Polym. Sci.* **2008**, *110*, 2305.
- Islam, M. S.; Pickering, K. L.; Foreman, N. J. *Comp. Part A* **2010**, *41*, 596.
- Sreekala, M. S.; Kumaran, M. G.; Thomas, S. *J. Appl. Polym. Sci.* **1997**, *66*, 821.
- Lai, S. M.; Liao, Y. C.; Chen, T. W. *Polym. Eng. Sci.* **2005**, *45*, 1461.
- Agrawal, R.; Saxena, N. S.; Sharma, K. B.; Thomas, S.; Sreekala, M. S. *Mater. Sci. Eng.* **2000**, *A277*, 77.
- Shibata, M.; Ozawa, K.; Teramoto, N.; Yosmiya, R.; Takeishi, H. *Macromol. Mater. Eng.* **2003**, *288*, 35.
- Lanzilotta, C.; Pipino, A.; Lips, D. *Proc. Annu. Tech. Conf. Soc. Plast. Eng.* **2002**, *60*, 2185.
- Bullions, T. A.; Gillespie, R. A.; Price-O'Brien, J.; Loos, A. C. *J. Appl. Polym. Sci.* **2004**, *92*, 3771.
- Bullions, T. A.; Hoffman, D.; Gillespie, R.; Price-O'Brien, J.; Loos, A. *Compos. Sci. Technol.* **2006**, *66*, 102.
- English, B. W.; Falk, R. H. Proceedings: Woodfiber-Plastic Composites: Virgin and Recycled Wood Fiber and Polymers for Composites; Forest Products Society: Madison, WI, **1995**; p 189.
- Kazayawoko, M.; Balatincez, J. J. Proceedings: Woodfiber-Plastic Composites Virgin and Recycled Wood Fiber and Polymers for Composites; Forest Products Society: Madison, WI, **1995**; p 81.
- Plackett, D. *J. Polym. Environ.* **2004**, *12*, 131.
- Beckermann, G. W.; Pickering, K. L.; Foreman, N. J. Proceedings of SPPM, Dhaka, Bangladesh, **2004**; p 257.
- Zhang, S. M.; Liu, J.; Zhou, W.; Cheng, L.; Guo, X. D. *Curr. Appl. Phys.* **2005**, *5*, 516.
- Ray, S. S.; Yamada, K.; Okamoto, M.; Ueda, K. *Polymer* **2003**, *44*, 857.
- Billmeyer, F. W. Jr. *Textbook of Polymer Science*, 3rd ed.; Wiley: New York, **1984**; Chapter 12.
- Huda, M. S.; Drzal, L. T.; Mohanty, A. K.; Misra, M. *Compos. Interf.* **2008**, *15*, 169.
- Krassig, H. A. *Polymer Monographs*, Vol. 2; Elsevier: New York, **1993**.
- Rana, A. K.; Mitra, B. C.; Banerjee, A. N. *J. Appl. Polym. Sci.* **1999**, *71*, 531.
- Fornes, T. D.; Paul, D. R. *Polymer* **2003**, *44*, 3945.